Appendix III:

Solid Solutions of Ni and Co Molybdates in Silica-dispersed and Bulk Catalysts prepared by Sol-gel, Impregnation and Citrate method: Characterization and Catalytic Activity in Propane Oxidative Dehydrogenation - Detailed Results -

III. Solid Solutions of Ni and Co Molybdates in Silica-dispersed and Bulk Catalysts prepared by Sol-gel, Impregnation and Citrate method: Characterization and Catalytic Activity in Propane Oxidative Dehydrogenation

III.1 Characterization of bulk Ni, Co and mixed Ni-Co molybdates prepared by the citrate method

III.1.1 Thermal behaviour

In the thermograms of almost all citrate gel precursors, a progressive weight loss of 73 % is observed between 373 and 873 K (see fig. III.1).

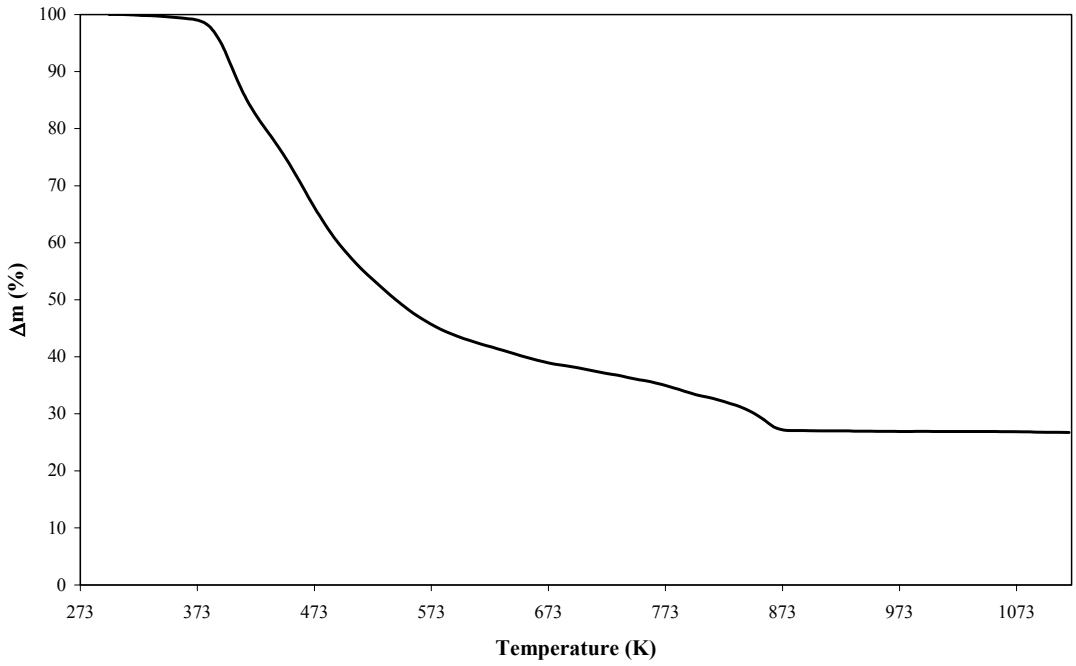

Fig.III.1: Thermogram of $Ni_{0.5}Co_{0.5}MoO_4$ prepared by the citrate method.

The chemical reactions which are involved in these degradation processes are related to the violent thermal decomposition of the citrate complexes upon oxidation in the presence of oxygen and nitric acid. The standard calcination conditions were fixed at 923 K (50 K higher than the final temperature in TGA) in a flow of 1 $l \cdot min^{-1}$ of dry air for 20 h, in order to ensure the complete decomposition of the citrate complexes.

III.1.2 X-ray photoelectron spectroscopy

The binding energies of the various elements were found in the following ranges: 855.5 ± 0.1 eV for $Ni2p_{3/2}$, 780.8 ± 0.1 eV for $Co2p_{3/2}$ and 232.2 ± 0.2 eV for $Mo3d_{5/2}$. These values correspond to the normally expected oxidation states (Ni(II), Co(II), Mo(VI)).

In $NiMoO_4$, the experimental atomic ratio (Ni/Mo) is far from the theoretical value corresponding to the bulk composition (0.29 with respect to 1.0); on the other hand, in $CoMoO_4$, the experimental ratio (Co/Mo) agrees quite well with the bulk composition (0.85 for 1.0). In $Ni_{0.5}Co_{0.5}MoO_4$ and $Ni_{0.45}Co_{0.55}MoO_4$, the experimental atomic ratio (Ni+Co/Mo) is equal to 0.6 for both analysed samples; an intermediate value between those in of $NiMoO_4$ and $CoMoO_4$. In these mixed Ni-Co molybdates, the atomic ratio (Ni/Co) is very close to the theoretical value, allowing us to conclude that the surface composition Ni/Co agrees well with the bulk composition. If we take into account the atomic ratio (Ni/Mo) and (Co/Mo), we observe values that are far from the theoretical ones: 0.26 and 0.37 for $Ni_{0.45}Co_{0.55}MoO_4$ with respect to 0.45 and 0.55 for the bulk composition, and 0.30 in both cases for $Ni_{0.5}Co_{0.5}MoO_4$ with respect to 0.5 in the bulk.

For $NiMoO_4$ and the solid solutions of $NiMoO_4$ and $CoMoO_4$, the experimental ratios (M/Mo) (M = Ni, Co) are far from those of the bulk composition, underlining the possible presence of MoO_3 on the surface, although this phase has been detected neither by XRD nor by Raman spectroscopy. In the citrate-prepared catalysts, carbon contamination is in the range of 23-28%, which is quite a lot.

III.1.3 Raman spectroscopy

Table III.1: Raman data of $Ni_{1-x}Co_xMoO_4$ obtained by the citrate method compared with reference data from the literature.

Compounds and References	Raman Shifts (cm^{-1})
α'-$NiMoO_4$	958 (vs), 909 (s), 703 (m), 383 (w), 258 (w), 174 (w), 139 (w)
$Ni_{0.75}Co_{0.25}MoO_4$	933* (vs), 881 (m), 811 (m), 701 (w), 365 (m), 338 (m)
$Ni_{0.50}Co_{0.50}MoO_4$	942* (vs), 883 (m), 811 (m), 698 (w), 362 (m), 332 (m)
$Ni_{0.45}Co_{0.55}MoO_4$	948-938 (vs), 884 (m), 819 (m), 700 (w), 363 (m), 334 (m)
$Ni_{0.40}Co_{0.60}MoO_4$	940* (vs), 880 (m), 811 (m), 700 (w), 366 (m), 338 (m)
$Ni_{0.35}Co_{0.65}MoO_4$	934* (vs), 880 (m), 811 (m), 700 (w), 361 (m), 339 (m)
$Ni_{0.25}Co_{0.75}MoO_4$	939* (vs), 882 (m), 811 (m), 700 (m), 365 (m), 338 (m)
β-$CoMoO_4$	928* (vs), 869 (m), 807 (m), 360 (m), 275 (w), 135 (w)
α-$NiMoO_4$ (103)	937, 915, 903 880, 806, 368, 358, 330
α'-$NiMoO_4$ (102,104)	962 (vs), 914 (s), 706 (m)
β-$NiMoO_4$ (103)	945 (vs), 935 (vs), 896 (s), 884 (m), 823 (s), 365 (s), 330 (s)
α-$CoMoO_4$ (103)	938 (vs), 915 (s), 880 (s), 815 (s), 700 (s), 476 (s), 362 (m), 330 (m)
β-$CoMoO_4$ (103)	943 (vs), 935 (vs), 896 (s), 882 (s), 818 (s), 363 (m), 330 (m)
MoO_3	994 (vs), 821 (vs), 664 (s), 289 (s), 281 (vs), 155 (s)

*) with a shoulder

III.1.4 UV-visible diffuse reflectance spectroscopy

In the Ni-Mo sample, the presence of α-$NiMoO_4$ (detected by XRD) is confirmed by the high energy band occurring below 480 nm, due to the $O^{2-} \rightarrow Mo^{6+}$ charge transfer (CT) process, characteristic of octahedrally coordinated Mo (111). Fig. III.2 displays the UV-vis. D.R. spectrum of $Ni_{0.5}Co_{0.5}MoO_4$; the maxima occurring at 525 and 580 nm are assigned to [CoO_6] octahedra (172). In all the DR spectra of $Ni_{1-x}Co_xMoO_4$ samples, a CT band starting at 480 nm appears, which is characteristic of the α-phase. Whereas XRD revealed in the case of $Ni_{0.5}Co_{0.5}MoO_4$ the presence of both α and β-phases, the UV-vis spectrum clearly shows the presence of the α-phase only, probably because the β-phase has been completely transformed to the α-phase upon sampling. It must be reminded that the tetrahedrally coordinated Mo (typical of the β-phase) (111), if present, would be identified by a high energy band below 440 nm, also due to the $O^{2-} \rightarrow Mo^{6+}$ charge transfer (CT) process.

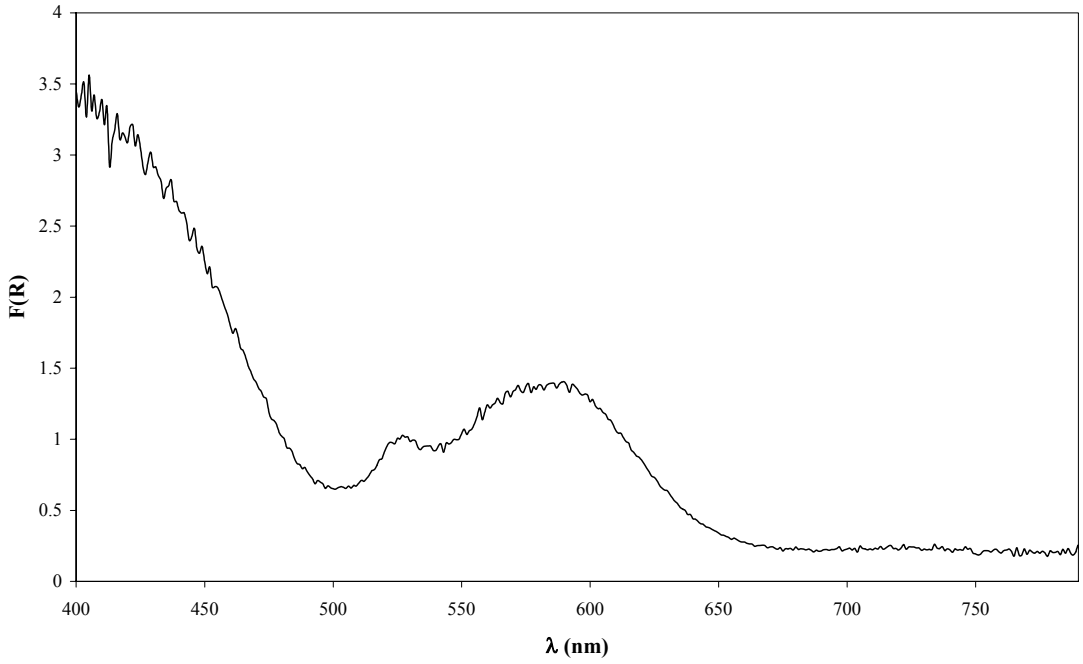

Fig.III.2: UV-vis diffuse reflectance spectrum (Kubelka-Munk function) of $Ni_{0.5}Co_{0.5}MoO_4$ prepared by the citrate method.

III.2 Characterization of silica-dispersed Ni, Co and mixed Ni-Co molybdates prepared by the sol-gel method

III.2.1 Thermal behaviour

All sol-gel precursors based on silica are characterized by the same TGA pattern, displaying two successive steps: the first abrupt one, between 373 K and 473 K, with a weight loss of 40 % is followed by a second one, more progressive, between 473 K and 1073 K, with a weight loss of 10 % (fig. III.3). When comparing with the citrate-prepared gels, the total weight loss in the sol-gel compounds is lower (50% vs 70%). The final temperature at the end of the second degradation step, is also higher (1073 K) than in the citrate method (873 K). A standard calcination temperature of 773 K for 20 hours in a flow of 1 $l \cdot min^{-1}$ of dry air has been selected for the sol-gel samples.

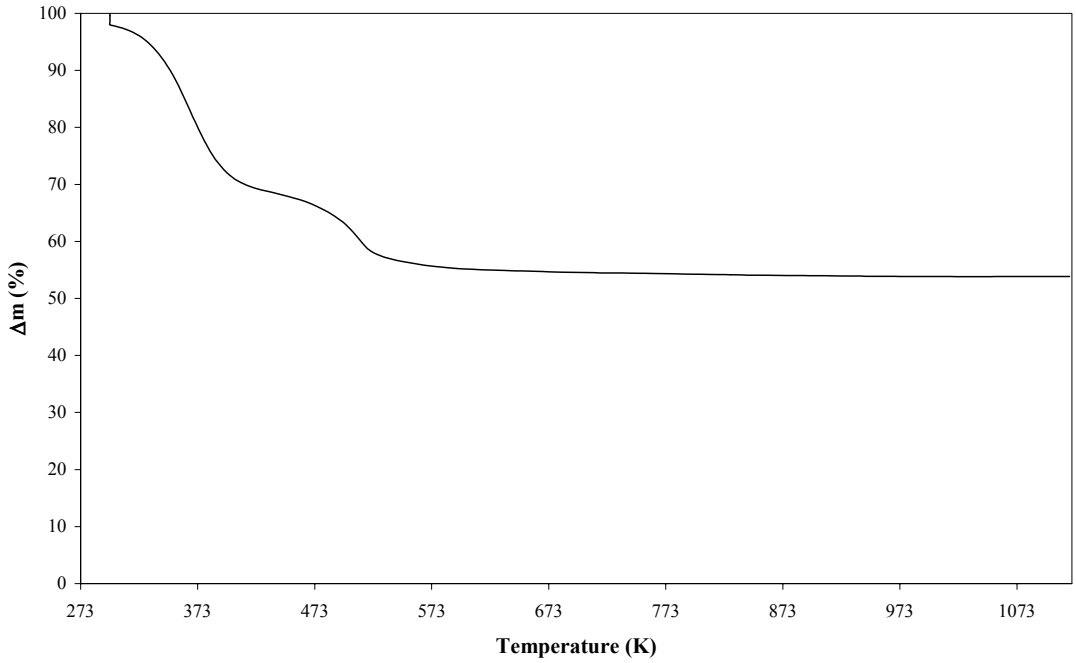

Fig.III.3: Thermogram of Ni:Co:Mo:Si (0.5:0.5:1:5) prepared by the sol-gel method.

III.2.2 X-ray diffraction and BET specific surface areas

Table III.2: Composition, specific surface area and crystalline phases detected in pure and mixed Ni-Co molybdates prepared by the sol-gel method (calcination at 773K).

Composition	Molar Ratio	S_{BET} ($m^2 \cdot g^{-1}$)[a)]	Detected crystalline phases
Ni:Mo:Si	1:1:20	327	β-$NiMoO_4$
Ni:Mo:Si	1:1:10	307	β-$NiMoO_4$
Ni:Mo:Si	1:1:5	216	β-$NiMoO_4$
Co:Mo:Si	1:1:20	322	β-$CoMoO_4$
Co:Mo:Si	1:1:10	294	β-$CoMoO_4$
Co:Mo:Si	1:1:5	217	β-$CoMoO_4$
Ni:Co:Mo:Si	0.75:0.25:1:20	441	β-$Ni_{0.75}Co_{0.25}MoO_4$
Ni:Co:Mo:Si	0.75:0.25:1:10	324	β-$Ni_{0.75}Co_{0.25}MoO_4$
Ni:Co:Mo:Si	0.75:0.25:1:5	241	β-$Ni_{0.75}Co_{0.25}MoO_4$
Ni:Co:Mo:Si	0.50:0.50:1:20	332	β-$Ni_{0.50}Co_{0.50}MoO_4$
Ni:Co:Mo:Si	0.50:0.50:1:10	295	β-$Ni_{0.50}Co_{0.50}MoO_4$
Ni:Co:Mo:Si	0.50:0.50:1:5	219	β-$Ni_{0.50}Co_{0.50}MoO_4$
Ni:Co:Mo:Si	0.25:0.75:1:20	352	β-$Ni_{0.25}Co_{0.75}MoO_4$
Ni:Co:Mo:Si	0.25:0.75:1:10	298	β-$Ni_{0.25}Co_{0.75}MoO_4$
Ni:Co:Mo:Si	0.25:0.75:1:5	254	β-$Ni_{0.25}Co_{0.75}MoO_4$

[a)] measurements with N_2 at 77 K; ± 1 m^2g^{-1};

III.2.3 Specific surface area and porosity measurements

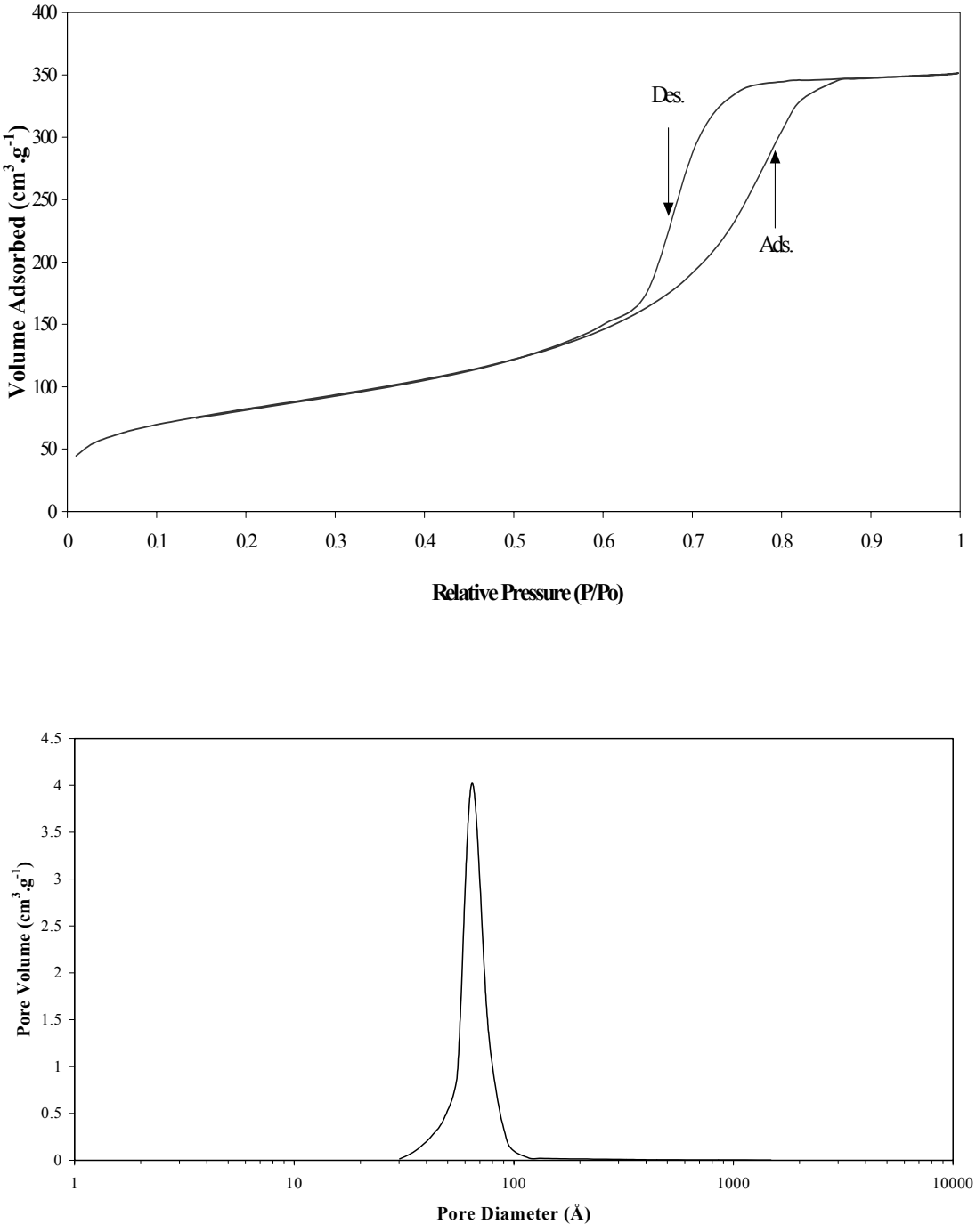

Fig.III.4: (a) Nitrogen adsorption-desorption isotherms and (b) pore size distribution from the BJH desorption curve of $Ni_{0.25}Co_{0.75}MoO_4/SiO_2$ (Si/Mo = 10) prepared by the sol-gel method.

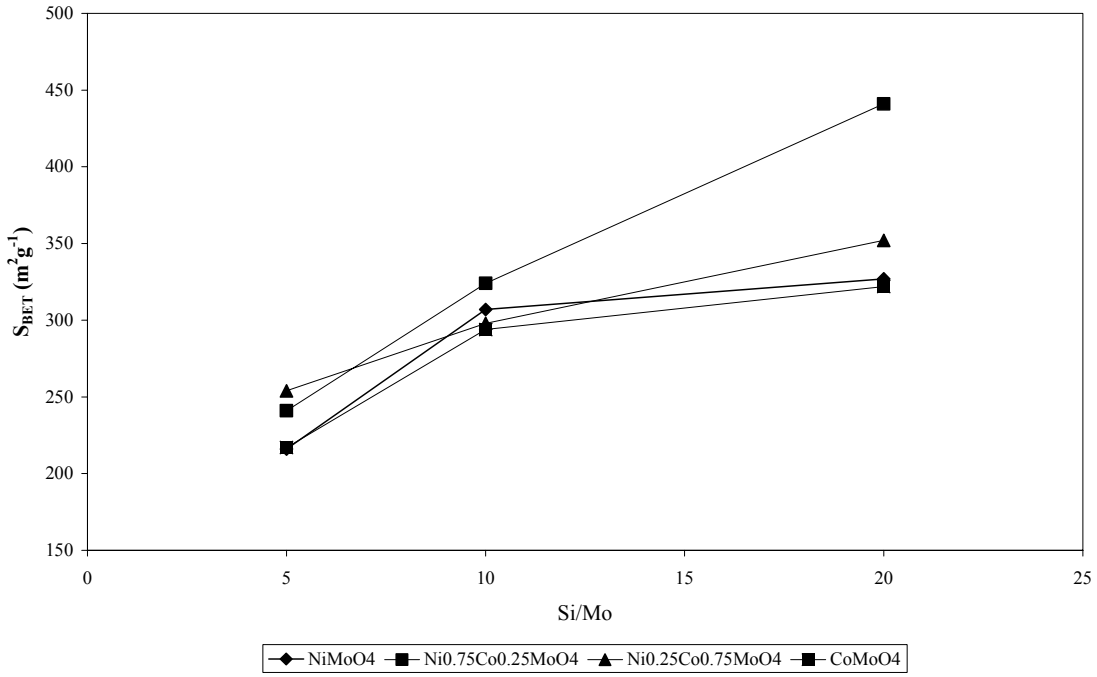

Fig.III.5: Evolution of the specific surface areas of $Ni_{1-x}Co_xMoO_4/SiO_2$ with respect to the amount of silicon (Si/Mo).

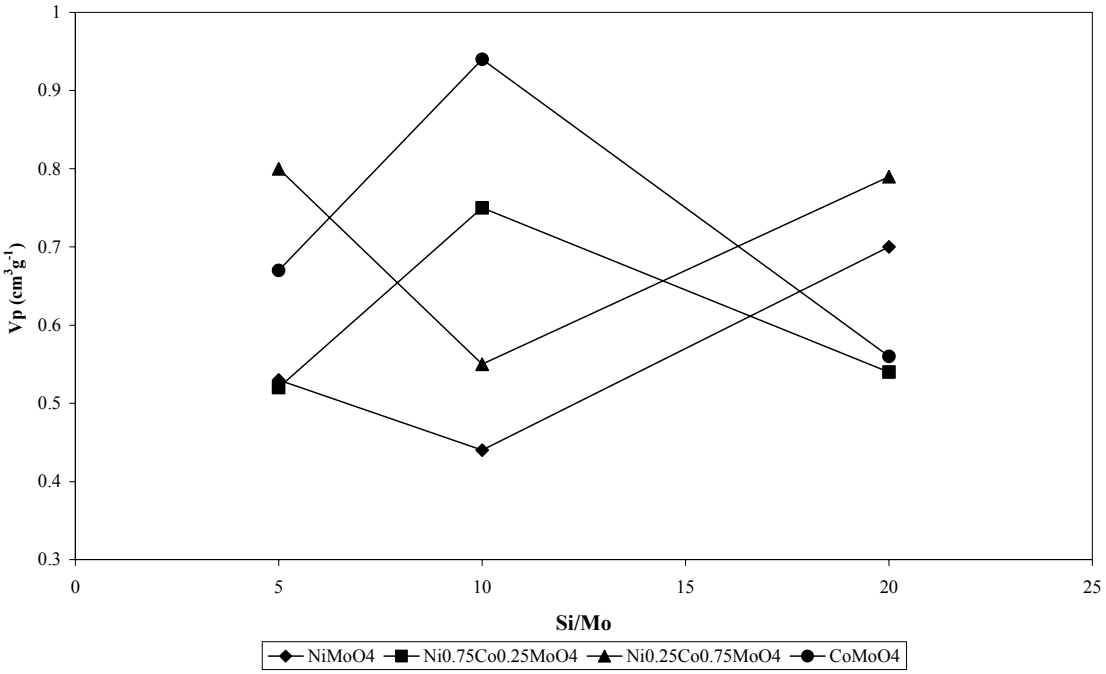

Fig.III.6: Evolution of the pore volume of $Ni_{1-x}Co_xMoO_4/SiO_2$ with respect to the amount of silicon (Si/Mo).

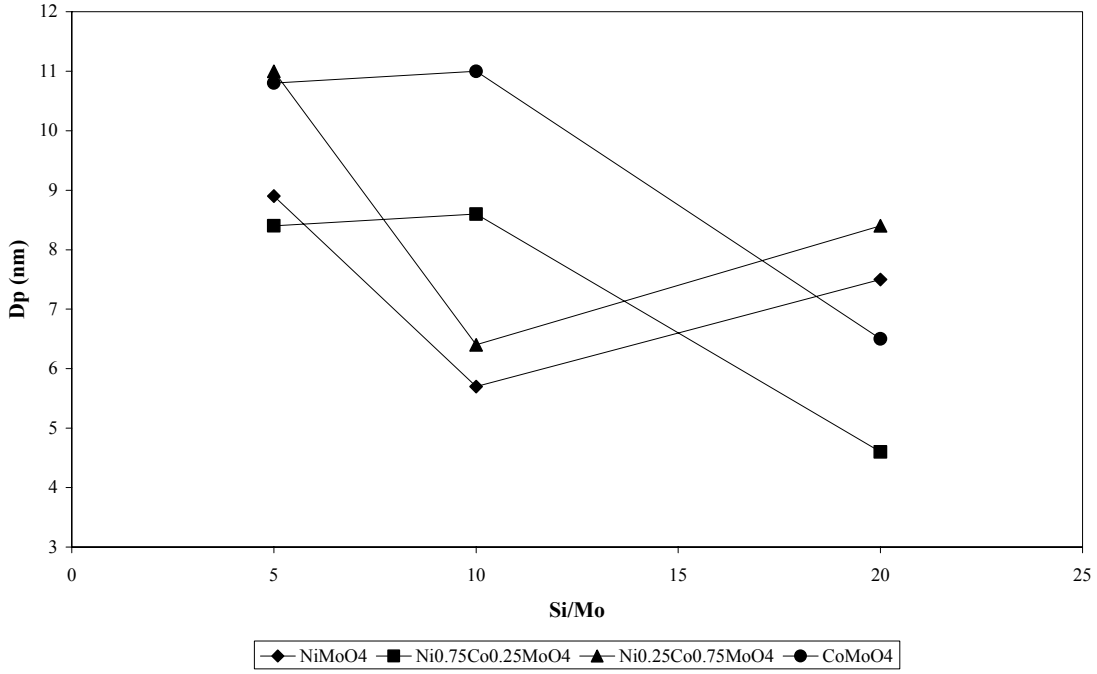

Fig.III.7: Evolution of the pore diameter of $Ni_{1-x}Co_xMoO_4/SiO_2$ with respect to the amount of silicon (Si/Mo).

III.2.4 Raman spectroscopy

Table III.3: Raman data of silica-dispersed Ni-Co molybdates obtained by the sol-gel method.

Composition	Molar Ratio	Raman Shifts (cm^{-1})
Ni:Mo:Si	1:1:20	958-946 (vs), 900 (w), 825 (m)
Ni:Mo:Si	1:1:10	956-946 (vs), 900 (m), 822 (w)
Ni:Mo:Si	1:1:5	955-945 (vs), 900 (m), 827 (m)
Co:Mo:Si	1:1:20	948-938 (vs), 875 (w), 812 (m), 684 (m), 478 (m)
Co:Mo:Si	1:1:10	933* (vs), 875 (w), 811 (m), 679 (m), 473 (w)
Co:Mo:Si	1:1:5	925* (vs), 869 (w), 811 (m), 662 (w)
Ni:Co:Mo:Si	0.75:0.25:1:20	957-946 (vs), 900 (m), 826 (m)
Ni:Co:Mo:Si	0.75:0.25:1:10	990 (s), 953-942 (s), 896 (w), 820 (vs), 664 (w)
Ni:Co:Mo:Si	0.75:0.25:1:5	955-944 (vs), 894 (s), 824 (s)
Ni:Co:Mo:Si	0.50:0.50:1:20	950-941 (vs), 890 (m), 822 (m), 590 (w)
Ni:Co:Mo:Si	0.50:0.50:1:10	992 (m), 945-936 (vs), 885 (m), 817 (s)
Ni:Co:Mo:Si	0.50:0.50:1:5	991 (w), 946-936 (vs), 886 (m), 811 (m)
Ni:Co:Mo:Si	0.25:0.75:1:20	985 (w), 929* (vs), 871 (w), 811 (m)
Ni:Co:Mo:Si	0.25:0.75:1:10	947-938 (vs), 880 (m), 820 (s)
Ni:Co:Mo:Si	0.25:0.75:1:5	935* (vs), 879 (m), 816 (s)

*) = with a shoulder

III.3 Characterization of silica-supported Ni-Co molybdates prepared by impregnation method

III.3.1 X-ray diffraction and specific surface areas

Table III.4 lists all the silica-supported catalysts prepared by impregnation with their respective BET specific surface areas and the crystalline phases identified by X-ray diffraction.

Table III.4: Composition, specific surface area and crystalline phases detected in SiO_2-supported mixed Ni-Co molybdates prepared by impregnation.

Composition	Molar Ratio	Detected Crystalline Phases	S_{BET} ($m^2 g^{-1}$)
Ni :Mo :Si	1:1 :5	β-$NiMoO_4$	196
Ni :Co :Mo :Si	0.75:0.25:1:5	β-$Ni_{0.75}Co_{0.25}MoO_4$	183
Ni :Co :Mo :Si	0.5:0.5:1:5	β-$Ni_{0.5}Co_{0.5}MoO_4$	194
Ni :Co :Mo :Si	0.25:0.75:1:5	β-$Ni_{0.25}Co_{0.75}MoO_4$	180
Co :Mo :Si	1:1 :5	β-$CoMoO_4$	171

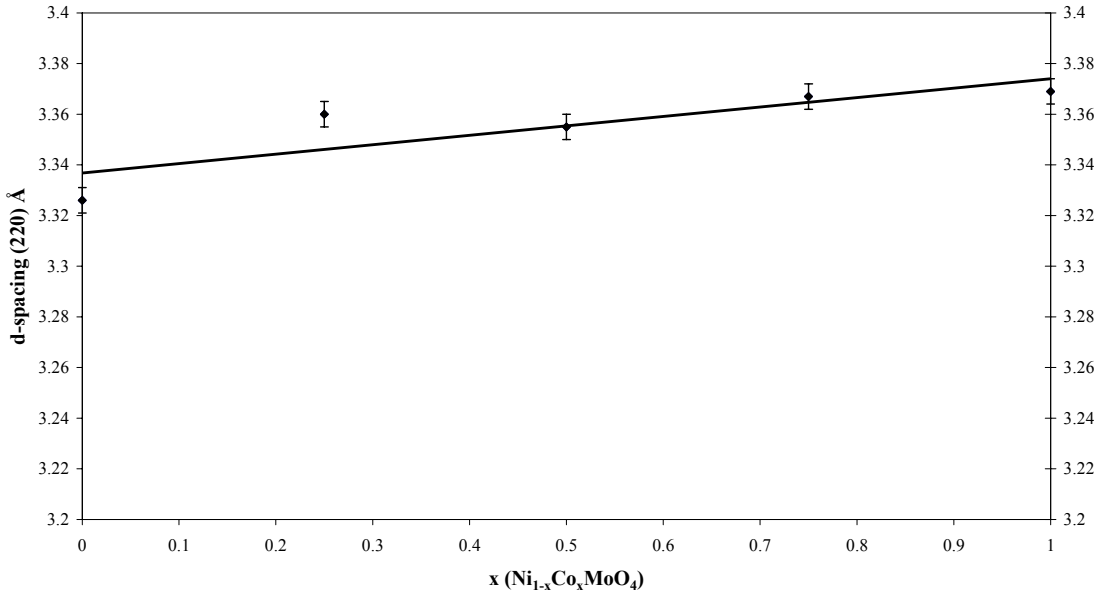

Fig.III.8: Verification of Vegard's law with the interreticular (220) d-spacing in silica-supported $Ni_{1-x}Co_xMoO_4$, prepared by impregnation (Si/Mo = 5).

As already observed for the analogous catalysts prepared by the sol-gel method, also in this case Vegard's law is observed (fig.III.8) and led us to conclude that the structures of these mixed Ni-Co molybdates are solid solutions of β-$NiMoO_4$ and β-

$CoMoO_4$. When Co substitutes for Ni along the series, a lattice expansion is observed as indicated by the shift of the (220) d-spacing from 3.326 Å to 3.369 Å.

III.3.2 Specific surface area and porosity measurements

Table III.5: Textural properties of some silica-supported $Ni_{1-x}Co_xMoO_4$ prepared by impregnation method.

Composition	Molar ratio	Type of isotherm	Vp ($cm^3\ g^{-1}$)[a]	Dp (nm)[b]
Ni:Mo:Si	1:1:5	IV	0.535	9.97
Ni:Co:Mo:Si	0.75:0.25:1:5	IV	0.488	9.67
Co:Mo:Si	1:1:5	IV	0.476	9.92

[a)] Average pore volume; [b)] Average pore diameter

III.3.3 Raman spectroscopy

Raman spectroscopy just confirms what XRD already revealed. All bands present in the Raman spectra and listed in table III.6 can be attributed to the β-phase.

Table III.6: Raman data of some silica-supported Ni-Co molybdates obtained by impregnation.

Composition	Molar Ratio	Raman Shift (cm^{-1})
Ni :Mo :Si	1:1 :5	957-944 (vs), 900-992 (s), 827 (s), 385-368 (m), 348 –337 (m)
Ni :Co :Mo :Si	0.5:0.5:1:5	951-942 (vs), 886 (m), 821 (m), 648 (w), 366 (m), 338 (m)
Co :Mo :Si	1:1 :5	932 (s), 869 (w), 811 (w), 680 (vs), 610 (m), 511 (m), 473 (vs), 364 (w)

III.3.4 X-ray photoelectron spectroscopy

In the catalysts prepared by impregnation, the binding energies of the various elements were found in the following ranges: 856.1 ± 0.1 eV for $Ni2p_{3/2}$, 781.3 ± 0.2 eV for $Co2p_{3/2}$, 103.8 ± 0.1 eV for Si2p. These values are very close to those of corresponding sol-gel prepared catalysts. The XPS spectra of molybdenum (fig. III.9) are resolved into two doublets corresponding to molybdenum present in two different oxidation states: 232.9 ± 0.2 eV for $Mo^{(VI)}3d_{5/2}$ and 231.9 ± 0.1 eV for $Mo^{(V)}3d_{5/2}$ (173). The average value of the experimental ratio (Mo(VI)/Mo) is equal to 0.74 ± 0.03.

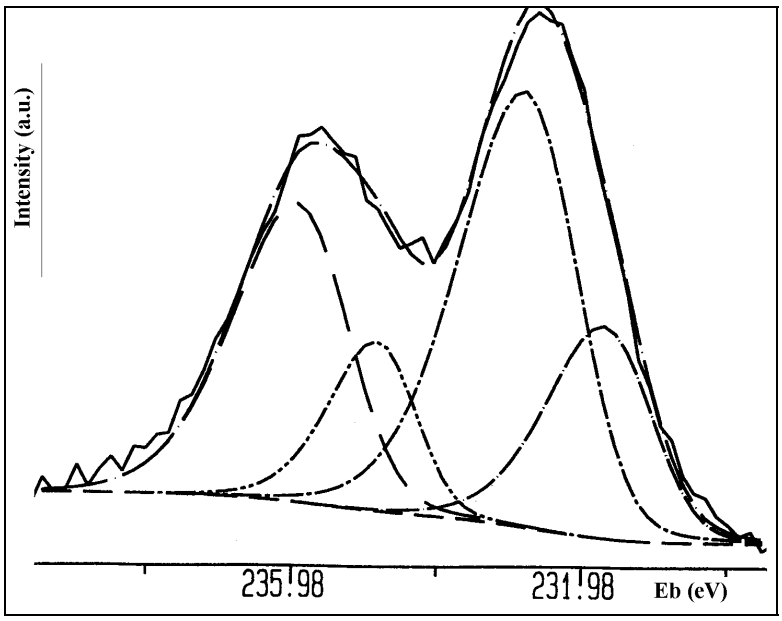

Fig.III.9: Mo 3d XPS spectrum of silica-supported $NiMoO_4$ (Si/Mo = 5), showing both Mo(VI) (Eb Mo $3d_{5/2}$ = 233.1eV) and Mo(V) (Eb Mo $3d_{5/2}$ = 232 eV).

Table III.7: Relative atomic intensity ratios measured by XPS in the silica-supported Ni-Co molybdates prepared by impregnation.

Composition and Molar Ratio	Ni/Mo		Co/Mo		Ni/Co		Ni/Si		Co/Si		Mo/Si	
	Exp.	Th.	Exp.	Th.	Exp.	Th.	Exp.	Th.	Exp.	Th.	Exp.	Th.
Ni :Mo :Si 1:1:5	0.44	1	-	-	-	-	0.034	0.2	-	-	0.076	0.2
Ni :Co :Mo :Si 0.75:0.25:1:5	0.49	0.75	0.18	0.25	2.75	3	0.05	0.15	0.02	0.05	0.11	0.2
Ni :Co:Mo :Si 0.5:0.5:1:5	0.39	0.5	0.4	0.5	0.98	1	0.03	0.1	0.03	0.1	0.077	0.2
Ni :Co:Mo :Si 0.25:0.75:1:5	0.26	0.25	0.43	0.75	0.62	0.33	0.025	0.05	0.04	0.15	0.093	0.2
Co :Mo :Si 1:1:5	-	-	0.42	1	-	-	-	-	0.035	0.2	0.084	0.2

III.4 Catalytic results

III.4.1 General comments and comparison bulk/supported catalysts

In a blank test performed with a sample of pure silica prepared by sol-gel method and calcined at 1073 K, conversion of propane on the support was found to start at 793 K.

$NiMoO_4$, $Ni_{0.5}Co_{0.5}MoO_4$ and $Ni_{0.25}Co_{0.75}MoO_4$ prepared by the citrate method were found to display an extremely low catalytic activity in propane ODH, the only product observed being CO_2. This result is obviously due to the very low specific surface areas obtained in that case ($S_{BET} < 13\ m^2g^{-1}$).

The catalytic performances of the silica dispersed Ni (Co) Mo-catalysts are presented in the tables III.8-11 according to their loading of active phase (5,10 or 20 mol Si/mol Mo). The evolution of the intrinsic yields in CO_2 for the different series of catalysts as a function of the Ni/Co composition is illustrated in the figures III.10 to III.13. It is clear that all sol-gel catalysts are characterized by better catalytic performances than the corresponding ones prepared as bulk phases by the citrate method. Dispersion of these molybdates improves therefore definitely their catalytic behaviour.

Table III.8: Catalytic results in propane ODH for silica-dispersed Ni-Co-molybdates ((Mo/Si) =1/20 mol/mol, 15 wt. % active phase)) prepared by the sol-gel method.

Catalyst Composition and S_{BET} ($m^2\ g^{-1}$)	Temp. (K)	$XC_3°$ (%)	$YC_3^=$ (%)	$Y*C_3^=$ (% m^{-2})	$SC_3^=$ (%)	XO_2 (%)	$YCO_2/3$ (%)	$Y*CO_2/3$ (% m^{-2})	SCO_2 (%)	C Balance
Ni-Mo-Si	723	2.1	1.0	0.012	47.0	2.4	0.7	0.0086	34.7	82 %
1:1:20 (327)	753	3.1	2.2	0.027	69.4	7.0	1.2	0.015	37.2	≈ 100 %
Ni-Mo-Si[a] 1:1:20 (188)	753	2.3	1.2	0.025	51.3	3.6	0.2	0.00425	9.0	60 %
Ni-Co-Mo-Si	673	1.2	0.4	0.0036	37.0	3.2	0.5	0.0045	43.6	81 %
0.75:0.25:1:20	723	3.1	1.5	0.0136	49.5	6.1	1.0	0.0091	33.1	83 %
(441)	753	4.9	2.5	0.023	50.2	9.7	1.4	0.0127	29.2	79 %
Ni-Co-Mo-Si 0.5:0.5:1:20 (332)	673	2.1	1.4	0.017	65.3	5.0	0.4	0.0048	16.6	82 %
	753	5.4	4.5	0.054	83.8	15.8	1.4	0.017	26.3	≈ 100 %
Ni-Co-Mo-Si	673	4.0	2.0	0.023	52.7	9.1	1.5	0.017	38.4	91 %
0.25:0.75:1:20	723	8.1	3.9	0.044	48.5	21.7	3.7	0.042	45.2	94 %
(352)	753	12.0	5.4	0.061	44.7	28.7	4.7	0.053	39.5	84 %
Co-Mo-Si 1:1:20 (322)	753	13.6	2.8	0.035	20.7	17.0	2.3	0.029	16.9	38 %
Co-Mo-Si[a]	723	0.8	0.3	0.0053	35.6	4.3	0.4	0.007	52.3	88 %
1:1:20 (227)	753	1.4	0.6	0.0105	41.2	6.2	0.7	0.012	51.0	92 %

a) = sample calcined at 1073 K

Table III.9: Catalytic results in propane ODH for silica-dispersed Ni-Co-molybdates ((Mo/Si) =1/10 mol/mol, 27 wt. % active phase)) prepared by the sol-gel method.

Catalyst Composition and S_{BET} (m^2 g^{-1})	Temp. (K)	$XC_3°$ (%)	$YC_3^=$ (%)	$Y*C_3^=$ (% m^{-2})	$SC_3^=$ (%)	XO_2 (%)	$YCO_2/3$ (%)	$Y*CO_2/3$ (% m^{-2})	SCO_2 (%)	C Balance
Ni-Mo-Si 1:1:10 (307)	673	2.0	0.9	0.012	46.3	6.5	1.1	0.014	52.7	99 %
	723	6.7	2.6	0.034	38.5	16.8	2.3	0.030	34.4	73 %
	753	11.0	4.1	0.053	36.8	23.8	3.2	0.042	28.8	66 %
Ni-Co-Mo-Si 0.75:0.25:1:10 (324)	723	4.4	3.3	0.041	74.4	9.1	1.1	0.0136	26.2	100 %
	753	8.2	4.7	0.058	57.0	15.8	1.8	0.022	22.4	79 %
Ni-Co-Mo-Si 0.5: 0.5:1:10 (295)	723	7.2	3.1	0.042	43.4	7.5	0.7	0.0095	9.1	53 %
	753	10.0	4.7	0.064	46.7	13.0	1.1	0.015	11.1	58 %
Ni-Co-Mo-Si 0.25:0.75:1:10 (298)	723	3.8	2.6	0.035	69.2	12.0	1.5	0.02	40.0	≈ 100 %
	753	6.5	4.2	0.056	64.6	15.5	2.2	0.03	33.7	98 %
Co-Mo-Si 1:1:10 (294)	673	2.0	1.0	0.014	44.2	3.6	0.6	0.0082	26.2	70 %
	723	5.5	2.8	0.038	51.0	10.4	1.7	0.023	32.0	83 %
	753	9.0	4.3	0.059	47.7	20.6	2.8	0.038	31.0	79 %

Table III.10: Catalytic results in propane ODH for silica-dispersed Ni-Co-molybdates ((Mo/Si) =1/5 mol/mol, 42 wt. % active phase)) prepared by the sol-gel method.

Catalyst Composition and S_{BET} (m^2 g^{-1})	Temp. (K)	$XC_3°$ (%)	$YC_3^=$ (%)	$Y*C_3^=$ (% m^{-2})	$SC_3^=$ (%)	XO_2 (%)	$YCO_2/3$ (%)	$Y*CO_2/3$ (% m^{-2})	SCO_2 (%)	C Balance
Ni-Mo-Si 1:1:5 (216)	673	3.0	0.0	0.0	0.0	15.2	2.4	0.044	76.0	76 %
	723	8.6	2.5	0.046	28.7	26.0	4.2	0.077	49.2	78 %
	753	13.6	3.7	0.068	27.0	42.0	7.0	0.13	53.6	81 %
Ni-Co-Mo-Si 0.75: 0.25:1:5 (241)	723	5.4	4.5	0.075	83.6	11.0	1.4	0.023	25.4	≈ 100%
	753	10.4	6.6	0.11	62.0	19.7	2.2	0.037	20.8	83 %
Ni-Co-Mo-Si 0.5: 0.5:1:5 (219)	673	2.8	2.1	0.038	75.3	4.6	0.3	0.0055	11.5	87 %
	723	7.4	4.9	0.089	65.7	11.2	0.8	0.0146	11.1	77 %
	753	11.7	6.9	0.126	59.2	20.7	1.4	0.026	12.1	71 %
Ni-Co-Mo-Si 0.25:0.75:1:5 (254)	753	12.8	7.0	0.11	55.8	38.0	7.0	0.11	55.0	≈ 100%
Co-Mo-Si 1:1:5 (217)	673	2.1	0.9	0.017	40.7	5.0	0.8	0.015	38.0	79 %
	723	5.2	2.9	0.053	55.5	13.6	2.2	0.042	44.0	99 %
	753	9.4	4.6	0.085	49.2	20.0	3.2	0.059	33.5	83 %

Table III.11: Catalytic results in propane ODH for silica-supported Ni-Co-molybdates ((Mo/Si) =1/5 mol/mol, 42 wt. % active phase)) prepared by impregnation.

Catalyst Composition and S_{BET} ($m^2\ g^{-1}$)	Temp. (K)	$XC_3°$ (%)	$YC_3^=$ (%)	$Y*C_3^=$ (% m^{-2})	$SC_3^=$ (%)	XO_2 (%)	$YCO_2/3$ (%)	$Y*CO_2/3$ (% m^{-2})	SCO_2 (%)	C Balance
Ni:Mo:Si 1:1:5 (196)	723	9.2	0.7	0.014	7.4	39.2	7.8	0.16	85.6	93 %
	753	19.6	0.4	0.008	2.2	76.4	11.4	0.23	58.3	61 %
Ni:Co:Mo:Si 0.5: 0.5:1:5 (194)	753	6.4	4.1	0.084	64.7	14.3	2.0	0.041	30.5	95 %
Ni:Co:Mo:Si 0.25: 0.75:1:5 (180)	673	3.1	1.9	0.04	61.1	3.9	0.4	0.0089	12.7	74 %
	723	7.8	4.6	0.1	59.0	10.3	1.3	0.029	16.1	75 %
	753	9.9	6.8	0.15	68.8	18.1	2.1	0.047	21.7	91 %
Co:Mo:Si 1:1:5 (171)	673	2.3	0.9	0.021	39.3	8.5	1.5	0.035	66.4	≈ 100%
	723	4.2	2.1	0.05	51.5	12.5	2.0	0.047	48.0	100 %
	753	7.2	3.9	0.09	54.5	15.6	2.4	0.056	34.2	89 %

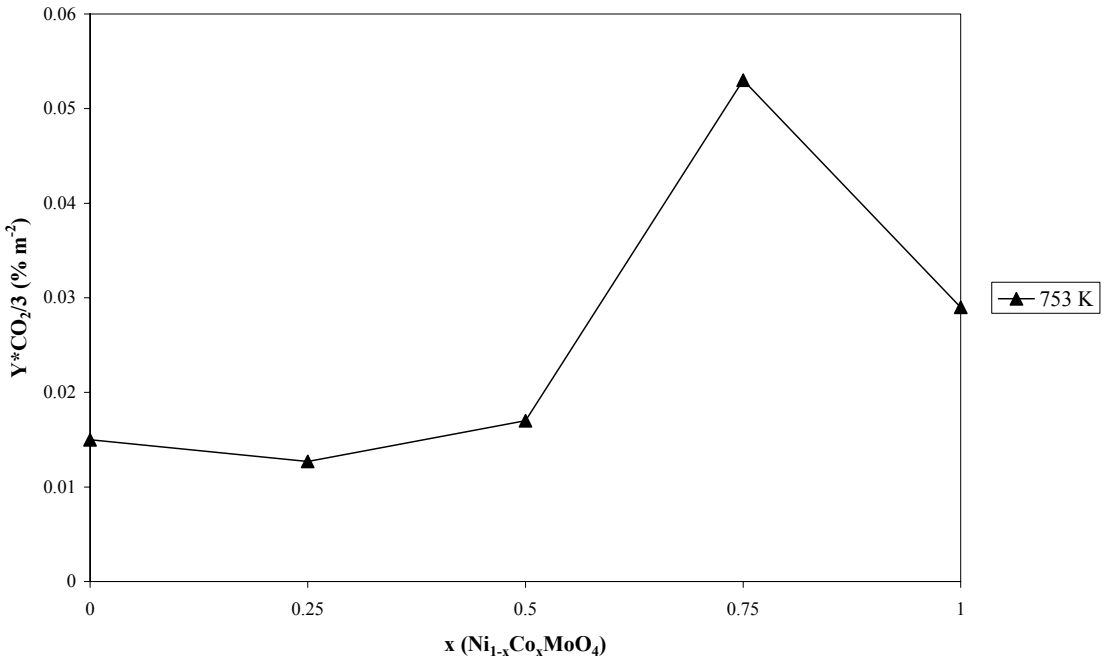

Fig.III.10: Evolution of the intrinsic CO_2 yield ($Y*CO_2/3$) in $Ni_{1-x}Co_xMoO_4/SiO_2$ (Si/Mo = 20), prepared by the sol-gel method.

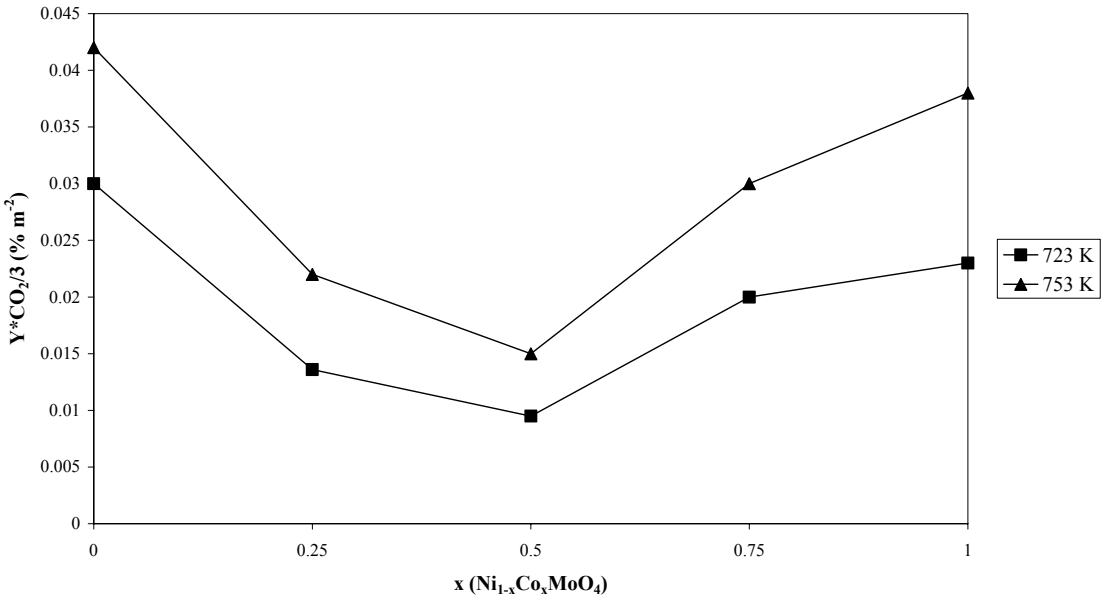

Fig.III.11: Evolution of the intrinsic CO_2 yield ($Y^*CO_2/3$) in $Ni_{1-x}Co_xMoO_4/SiO_2$ (Si/Mo = 10), prepared by the sol-gel method.

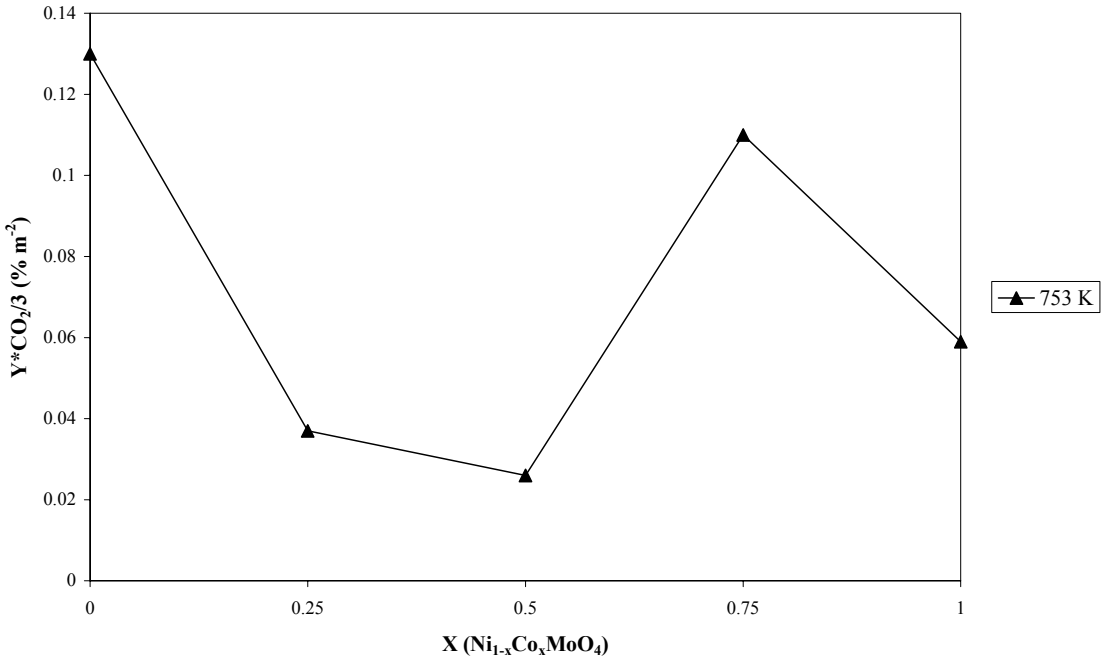

Fig.III.12: Evolution of intrinsic CO_2 yield ($Y^*CO_2/3$) in $Ni_{1-x}Co_xMoO_4/SiO_2$ (Si/Mo = 5), prepared by the sol-gel method.

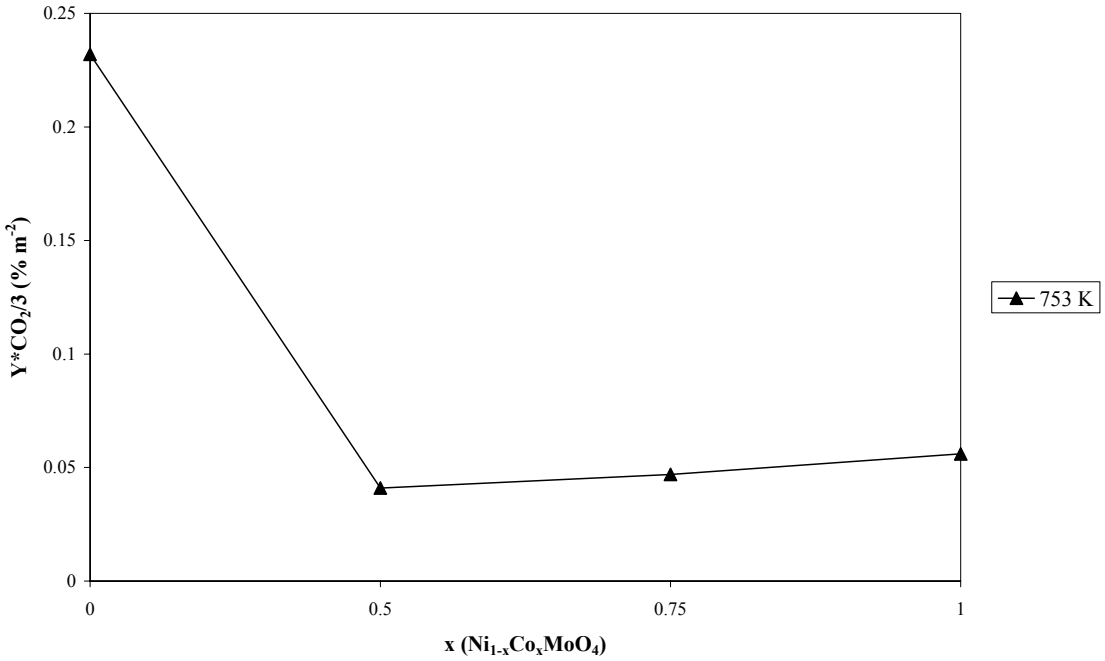

Fig.III.13: Evolution of the intrinsic CO_2 yield (Y*CO_2/3) in $Ni_{1-x}Co_xMoO_4/SiO_2$ (Si/Mo = 5), prepared impregnation.

III.4.2 Influence of Ni/Co composition

Let us first comment the data collected with the sol-gel made samples. In the case of Ni-Co-Mo-Si samples characterized by Si/Mo = 20, the maximum intrinsic propene yield is observed for the $Ni_{0.25}Co_{0.75}MoO_4$ sample (fig. III.17 in chapter III), but the catalyst also exhibits the highest intrinsic CO_2 yield (fig. III.10), according to the fact that it consumes the highest amount of oxygen. Next to it, $Ni_{0.5}C_{0.5}MoO_4$ is characterized by a higher Y*$C_3^=$ value but a lower Y*CO_2/3 than $CoMoO_4$.

When Ni-Co molybdates with Si/Mo = 10 are tested, the differences in catalytic behaviour between all molybdates are very small, it appears that all these catalysts behave in the same way. However, $Ni_{0.5}Co_{0.5}MoO_4$, is the catalyst with the highest intrinsic propene yield along the overall range of temperature, and at the same time that with the lowest intrinsic CO_2 yield (fig.III.11); the other two mixed Ni-Co molybdates have intrinsic propene yields very close to that of $CoMoO_4$ and they produce less CO_2 than $NiMoO_4$ or $CoMoO_4$: both simple molybdates show the highest intrinsic CO_2 yield and consume the highest amount of oxygen.

All mixed Ni-Co molybdates have higher propene intrinsic yields than $NiMoO_4$ and $CoMoO_4$. The highest consumption of oxygen is observed for $NiMoO_4$. Generally speaking, this series of catalysts is responsible for the conversion of the highest percentage of oxygen. In the case of silica-dispersed molybdates characterized by Si/Mo = 5, $Ni_{0.5}Co_{0.5}MoO_4$ showed the highest values of intrinsic propene yield (fig. III.19 in chapter III) and the minimum intrinsic CO_2 yield (fig. III.12): this is consistent with the rather low oxygen conversion of this catalyst.

Representative results obtained with the analogous catalysts prepared by impregnation are shown in fig.III.20 (chapter III) and fig.III.13, all the raw data being given in table III.11. $NiMoO_4$, even if very active ($XC_3° = 19.6$ % and $XO_2 = 76.4$ %, at 753 K) produces only CO_2 and very little amount of propene. All solid solutions of $NiMoO_4$ and $CoMoO_4$ display better propene yield (4.1 %, 5.7 % and 6.8 %) than the simple Ni or Co molybdates (0.4 % and 3.9 %, respectively). The most performing catalyst towards propene production is $Ni_{0.25}Co_{0.75}MoO_4$, but quite generally all solid solutions are more active than the simple Ni- or Co-molybdates. One of the most interesting characteristics of these catalysts prepared by impregnation is that they all give the same amount of CO_2 as by-product (fig. III.13), except for $NiMoO_4$: the differences in Ni/Co composition do not seem to influence the CO_2 intrinsic yield of these catalysts.

III.4.3 Influence of silica loading

Fig.III.14 illustrates the influence of active phase loading on silica on the intrinsic CO_2 yields, for all $Ni_{1-x}Co_xMoO_4$. In the case of $NiMoO_4$, it has been observed that the higher the loading of the active phase, the higher the intrinsic propene yield (at 723 and 753 K); on the other side the increasing loading of the active phase leads to high intrinsic propene yield and to very high intrinsic CO_2 yield values with consequent slightly low propene selectivities. Concerning Co-Mo-Si catalysts prepared by sol-gel method, increasing loadings of the active phase lead to similar increase of both intrinsic propene and CO_2 yields, with consequent slight increase of propene selectivity when going from higher to lower Si content.

Concerning silica-dispersed $Ni_{0.75}Co_{0.25}MoO_4$, an increasing silica content leads to a decreasing propane conversion ($XC_3° = 10.4 \rightarrow 4.9$ %) as well as a decreasing propene selectivity ($SC_3^{=} = 62 \rightarrow 50.2$ %). $Ni_{0.5}Co_{0.5}MoO_4$ shows an enhancement of

propane conversion when increasing the loading of the active phase ($XC_3° = 5.4 \rightarrow 11.7$ %) and it presents a minimum in propene selectivity when Si/Mo = 10.

The catalytic behaviour of $Ni_{0.25}Co_{0.75}MoO_4$ does not follow any specific trends: it presents a minimum in propane conversion at Si/Mo = 10 and a maximum in propene selectivity at the same Si/Mo ratio.

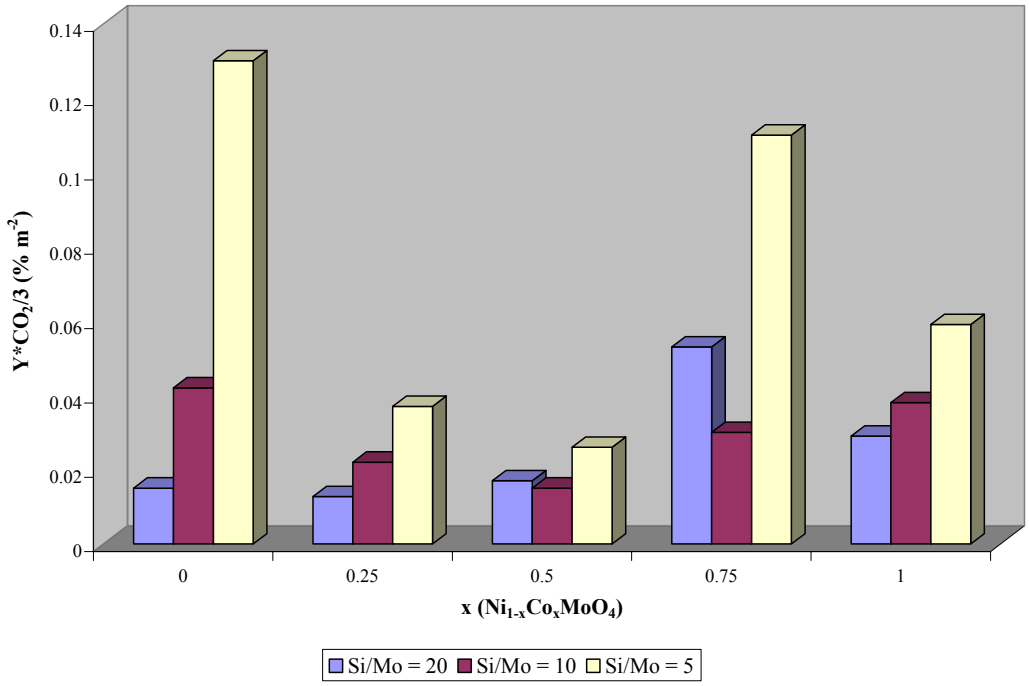

Fig.III.14: Effect of the silica loading in the evolution of the intrinsic CO_2 yield ($Y^*CO_2/3$) in SiO_2-dispersed $Ni_{1-x}Co_xMoO_4$.

III.4.4 On the catalytic performances of solid solutions of Ni and Co molybdates supported on silica

$NiMoO_4$, $CoMoO_4$ and the solid solution $Ni_{1-x}Co_xMoO_4$ display a good catalytic activity in propane ODH, even if Venezia and coworkers (154) generally noticed that with the introduction of the metals during the sol-gel synthesis, the embedding of the active species inside the silica matrix can lead to a decrease of the number of available active sites and consequently to a lower catalytic activity.

Mixed Ni-Co molybdates dispersed on SiO_2

The mixed $Ni_{1-x}Co_xMoO_4/SiO_2$ catalysts also display interesting catalytic performances: for x = 0.25, the catalyst generally behaves in the same way as $NiMoO_4$ in terms of propane conversion, meaning that a higher content of the active phase leads to high propane conversion, but it behaves like $CoMoO_4$ when looking at selectivity: the

higher the active phase loading, the higher the selectivity to propene. An increasing propene intrinsic yield is also found, which was already observed in the case of the simple Ni or Co molybdates.

The same behaviour is also observed in $Ni_{0.5}Co_{0.5}MoO_4$, but the main difference is that the selectivity towards propene does not follow any trend, and is completely independent from the silica content (even if an increasing content of the active phase always leads to higher $Y^*C_3^=$, as observed in all other cases).

Supported $Ni_{0.25}Co_{0.75}MoO_4$ behaves also independently from the silica content: the only general behavior observed is that for each temperature, the catalyst with (Si/Mo) = 10 presents a minimum for $XC_3°$ and for $Y^*C_3^=$. Among the three mixed Ni and Co molybdates, $Ni_{0.25}Co_{0.75}MoO_4$ is the one characterized by the highest $Y^*CO_2/3$ (see tables III.8-10).

$Ni_{1-x}Co_xMoO_4$ supported on SiO_2 prepared by impregnation method

Observing the silica supported catalysts prepared by impregnation method, $YC_3^=$ values of solid solutions as well as I.P.A and P.P. values are higher than those of the simple $NiMoO_4$ and $CoMoO_4$ (table III.12.). All these samples are characterized by the same pore diameter and by very close pore volume (Vp), which cannot explain the differences in the catalytic performances.

Table III.12: Intrinsic propene activity, propene productivity and pore diameter in silica supported Ni and Co molybdates, prepared by impregnation.

$Ni_{1-x}Co_xMoO_4$	Si/Mo = 5			
	I. P. A[a] ($\mu mol\ h^{-1}\ m^{-2}$)	P. P[b] ($mmol\ h^{-1}\ g_{ph}^{-1}$)	Vp ($cm^3\ g^{-1}$)	Dp (nm)
x = 0	0.60	0.28	0.535	9.97
x = 0.5	6.23	2.83	-	-
x = 0.75	11.13	4.69	-	-
x = 1	6.73	2.69	0.48	9.92

a) Intrinsic propene activity

b) Propene productivity

$Ni_{0.25}Co_{0.75}MoO_4$ prepared by sol-gel method displays a lower intrinsic propene yield and a higher CO_2 yield than those shown by the corresponding catalyst prepared by impregnation, even if the sol-gel sample shows a (Co/Mo) equal to that of the impregnated catalyst and a lower (Ni/Mo) ratio (0.09 and 0.26 for catalyst prepared by sol-gel and impregnation respectively). It must be pointed out that the differences in the catalytic behaviour could be explained in the different degree of the dispersion of the

metals on the surface of the catalyst: in fact, almost all (M/Si) ratios of $Ni_{0.25}Co_{0.75}MoO_4$ prepared by impregnation are higher (see table III.7): the metals are better dispersed and the active phase is therefore more active.

If we observe the (Ni/Co) experimental atomic ratio of the impregnated $Ni_{0.25}Co_{0.75}MoO_4$ catalyst, it is higher than that of the sol-gel analogous one (0.62 and 0.20 %, respectively). It seems that a higher experimental (Ni/Co) ratio leads to higher catalytic activity.